

# Secondary Metabolites of Onygenales Fungi Exemplified by *Aioliomyces pyridodomo*s

Zhenjian Lin,<sup>†</sup> Thomas B. Kakule,<sup>†</sup> Christopher A. Reilly,<sup>§,†</sup> Sinem Beyhan,<sup>‡,⊥</sup> and Eric W. Schmidt<sup>\*,†,§</sup>

<sup>†</sup>Department of Medicinal Chemistry, University of Utah, Salt Lake City, Utah 84112, United States

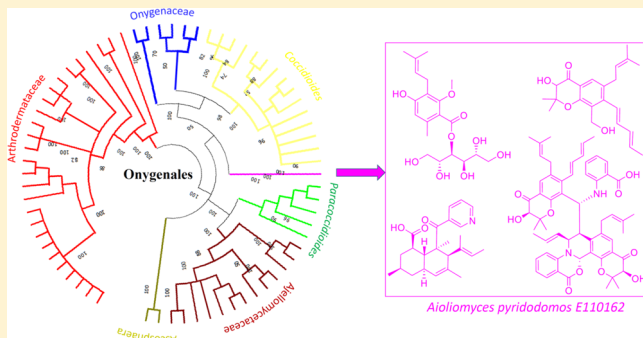
<sup>‡</sup>Department of Infectious Diseases, J. Craig Venter Institute, La Jolla, California 92037, United States

<sup>⊥</sup>Department of Medicine, University of California, San Diego, La Jolla, California 92093, United States

<sup>§</sup>Department of Pharmacology & Toxicology and Center for Human Toxicology, University of Utah, Salt Lake City, Utah 84112, United States

## S Supporting Information

**ABSTRACT:** Fungi from the order Onygenales include human pathogens. Although secondary metabolites are critical for pathogenic interactions, relatively little is known about Onygenales compounds. Here, we use chemical and genetic methods on *Aioliomyces pyridodomo*s, the first representative of a candidate new family within Onygenales. We isolated 14 new bioactive metabolites, nine of which are first disclosed here. Thirty-two specialized metabolite biosynthetic gene clusters (BGCs) were identified. BGCs were correlated to some of the new compounds by heterologous expression of biosynthetic genes. Some of the compounds were found after one year of fermentation. By comparing BGCs from *A. pyridodomo*s with those from 68 previously sequenced Onygenales fungi, we delineate a large biosynthetic potential. Most of these biosynthetic pathways are specific to Onygenales fungi and have not been found elsewhere. Family level specificity and conservation of biosynthetic gene content are evident within Onygenales. Identification of these compounds may be important to understanding pathogenic interactions.



Fungi produce secondary metabolites that establish and maintain infections.<sup>1</sup> For example, *Aspergillus fumigatus* (order Eurotiales) synthesizes gliotoxin as part of its repertoire to circumvent the human immune system.<sup>2</sup> Eurotiales fungi, such as *Aspergillus* spp. and *Penicillium* spp., are the best-studied producers of secondary metabolites, with thousands of known compounds including those important in virulence. In contrast, fungi from the order Onygenales include important human pathogens that are challenging to treat,<sup>3,4</sup> but much less is known about their secondary metabolites. Several Onygenales compounds from pathogens have been produced via heterologous expression,<sup>5,6</sup> but it remains unknown if these are produced in the native host. Similarly, an Onygenales biosynthetic gene cluster (BGC) implicated in virulence is an iron-sequestering siderophore pathway with unknown chemical products.<sup>7,8</sup>

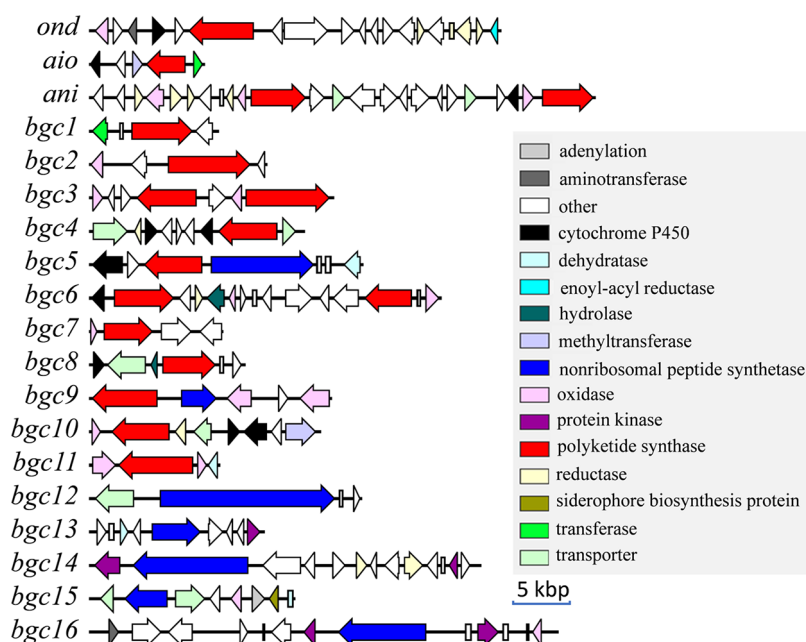
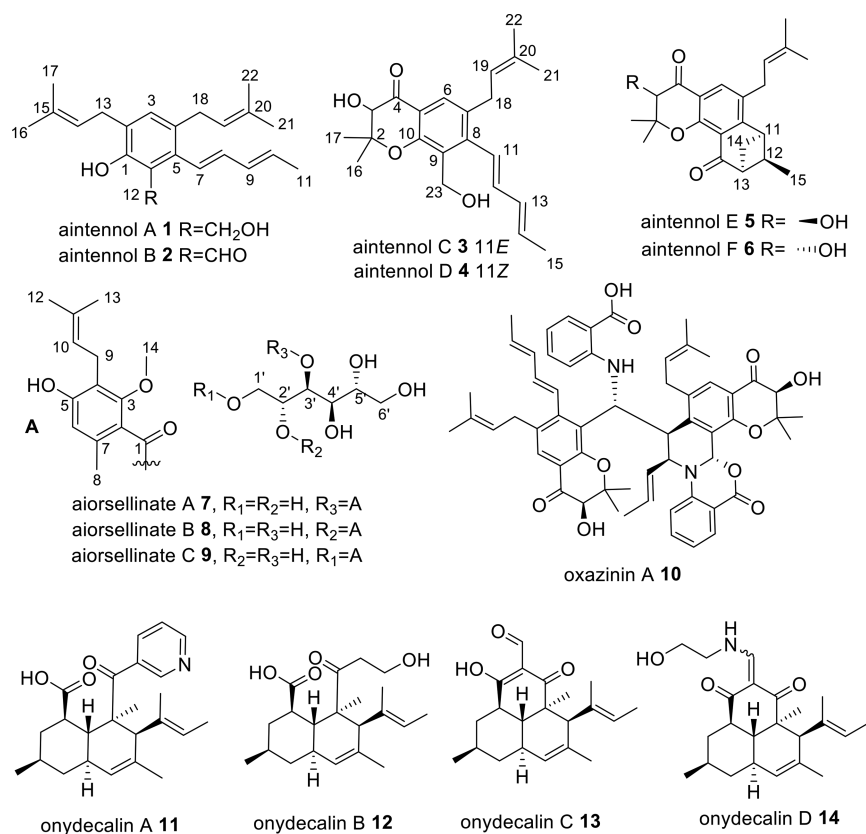
From nonpathogenic Onygenales, many compounds have been reported. A few examples include polyketides and isoprenoids from marine<sup>9</sup> and terrestrial Onygenales.<sup>10–15</sup> Onygenales and Eurotiales strains contain a similar number of BGCs responsible for producing secondary metabolites, although the types of genes differ slightly between the groups.<sup>16–19</sup> Thus, it might be expected that both pathogenic and nonpathogenic Onygenales provide a reservoir of new secondary metabolites important in infection.

Here, we examined *Aioliomyces pyridodomo*s, a nonpathogenic Onygenales isolate from a coral reef tunicate in the Eastern Fields of Papua New Guinea. Through genome sequencing, we analyzed BGC content of *A. pyridodomo*s and compared it to the available Onygenales genomes. This analysis revealed a large untapped diversity of Onygenales compounds awaiting discovery from both pathogenic and nonpathogenic isolates. Sequence analysis shows that the number of BGCs in Onygenales is similar to that found in Eurotiales, but encoding a different and new suite of compounds.

To determine the chemical potential of *A. pyridodomo*s, we performed fermentation and chemical analysis, leading to the discovery of 14 polyketides (1–14). Previously, we identified a new polyketide derivative, oxazin A (10), which exhibited activity against transient receptor potential (TRP) channels.<sup>20</sup> Subsequently, we described a series of unusual polyketides, onydecals (11–14), with anti-TRP and anti-*Histoplasma* activities.<sup>21</sup> Here, we describe further new polyketide structural families encompassing aintennols (1–6) and aiorsellinates (7–9). We identified some of the BGCs linked to *A. pyridodomo*s

**Received:** February 8, 2019

Chart 1

Figure 1. Predicted PKS and NRPS BGCs in the *A. pyridodimos* genome.

compounds by sequence analysis and heterologous expression. Our data suggest that Onygenales is a rich source of untapped secondary metabolites.

## RESULTS AND DISCUSSION

**Biosynthetic Pathways in *A. pyridodimos*.** *A. pyridodimos* E110162 was sequenced with Illumina HiSeq, providing

a draft genome with 526 scaffolds. Using the antiSMASH<sup>22</sup> algorithm with cluster finder,<sup>23</sup> we identified 86 putative BGCs in the genome. The contigs containing BGCs were manually examined to ensure that they contained the entire BGC and that BGCs did not span multiple scaffolds. We excluded the category “cf\_putative”, which are speculative BGC calls, leading to 32 BGCs belonging to well-defined secondary metabolic classes. We focused on the 19 polyketide and

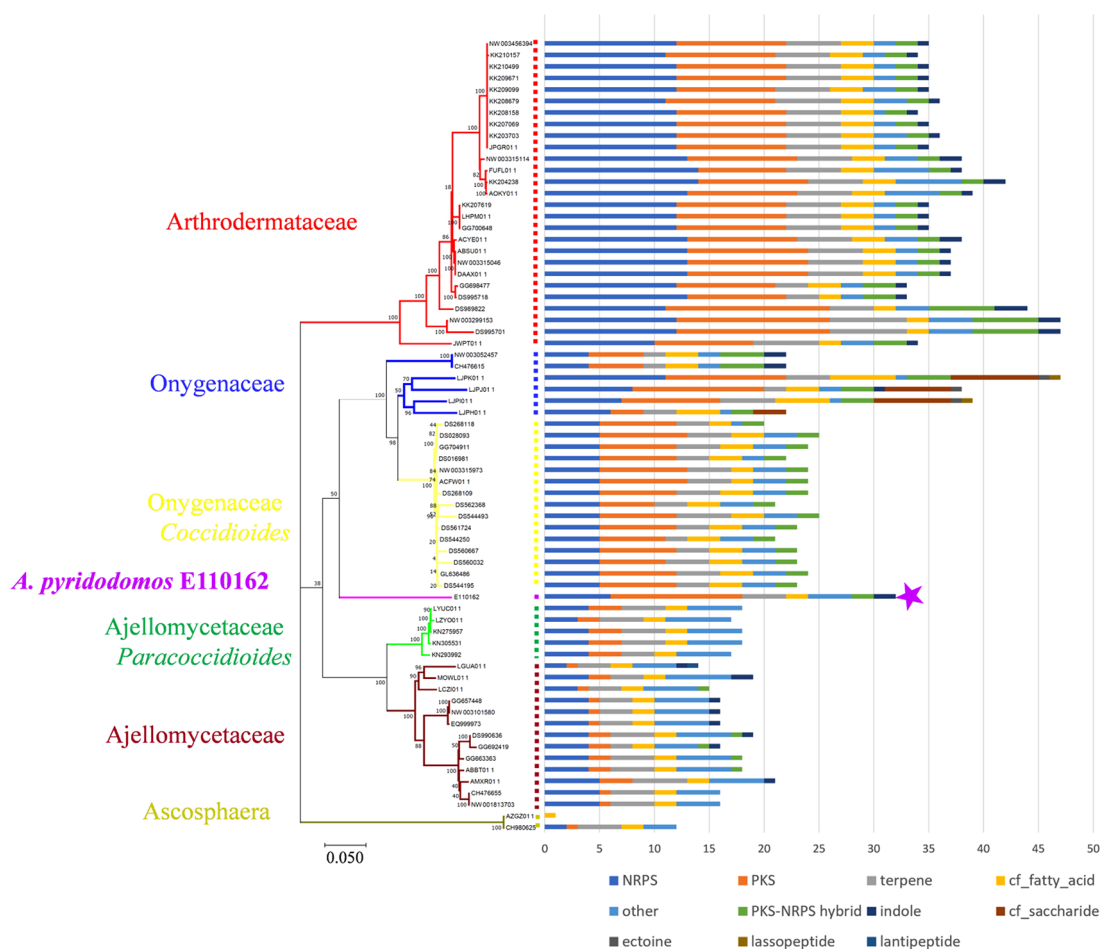


**Figure 2.** Onygenales contains a wealth of secondary metabolic BGCs. The purple star indicates *A. pyridodomo*. A phylogenetic tree (left) was obtained by concatenating 17 conserved proteins in 69 Onygenales strains with available genome sequences and performing a maximum-likelihood method with MEGA-X.<sup>27</sup> Bootstrap values are indicated at the nodes of the tree. Family level taxonomy is indicated, except for the important genera *Coccidioides* and *Paracoccidioides*, which belong to Ajellomycetaceae and Onygenaceae, respectively. antiSMASH was used to predict BGCs, which are enumerated in the bar chart at the right (excluding the antiSMASH category “cf\_putative”).

nonribosomal peptide metabolic BGCs (Figure 1), because these are important biosynthetic families in fungi with extensive experimental data.<sup>24,25</sup> Twelve BGCs contained at least one polyketide synthase (PKS), five contained a nonribosomal peptide synthetase (NRPS), and two contained a PKS and an NRPS. There were no hybrid PKS-NRPS genes<sup>26</sup> in the genome.

**Comparison with Other Fungal Genomes.** We sought to understand the *A. pyridodomo* genome in comparison to those in other Onygenales. We compared the identified *A. pyridodomo* BGCs to those from 68 sequenced Onygenales strains (Table S1) available in GenBank at the time of analysis. To obtain BGCs, we applied antiSMASH<sup>22</sup> to the 69 genomes to identify 1888 BGCs (excluding “cf\_putative”), of which 1184 contained a PKS, an NRPS, or both. These were overlaid on a maximum-likelihood phylogenetic tree of the 69 strains (Figure 2). As expected, >90% of the PKS genes belong to the vast group of fungal type I iterative PKSs.<sup>24</sup> Families Arthrodermataceae and Onygenaceae contain the most abundant BGCs, while the Ajellomycetaceae family contains relatively fewer. Ascospaera, which is deeply branched within the Onygenales tree, contains the fewest BGCs.

We next sought to determine whether the Onygenales BGCs were similar to those from other fungi. We focused on PKS and

NRPS clusters, which are the most straightforward to analyze. Using antiSMASH, we found that only 38 out of the 1184 BGCs had significant similarity (over 70% of the genes show similarity to known clusters) to BGCs from fungi outside of the Onygenales. These related BGCs were found in 17 strains from the order Eurotiales and 10 strains from class Sordariomycetes (Figure S1). Many of these 27 strains are plant or insect pathogens. Thus, while fungal PKS and NRPS genes share many common features, this analysis suggests that Onygenales encodes a unique suite of compounds in comparison to other fungi.

We asked how the Onygenales BGCs were distributed within the order, comparing the fungal taxonomic family to the biosynthetic Gene Cluster Family (GCF), as defined by Medema et al.<sup>28</sup> The concept of GCF was introduced so that whole biosynthetic pathways could be compared.<sup>29</sup> Using Medema’s method,<sup>28</sup> 1184 PKS and NRPS BGCs were classified into 103 GCFs and 119 singletons, for a total of 222 groups. We used two different methods, Cytoscape networking<sup>30</sup> and cluster analysis,<sup>28</sup> to graphically analyze the distribution of GCF in comparison to fungi at the family level (Figures 3 and S2). Both methods revealed that the majority of GCFs (96% of the 222) are specific to a single fungal family within Onygenales. Seven GCFs in the network are shared by

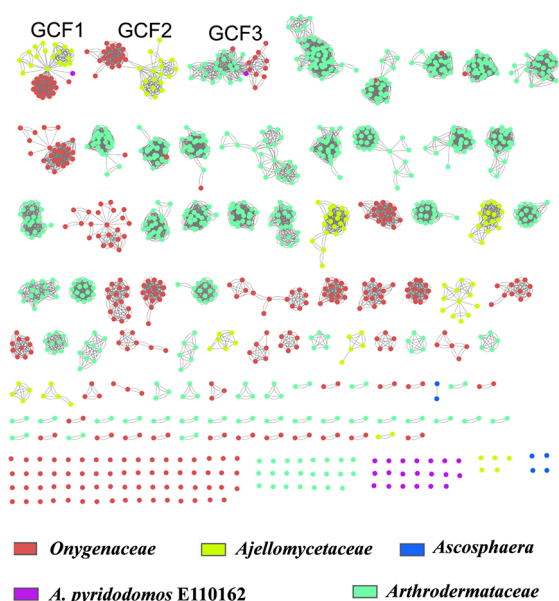


**Figure 3.** Cytoscape analysis reveals that most Onygenales biosynthetic pathways are specific to individual families of fungi. We identified 1184 PKS and NRPS BGCs, which are indicated by circles. Connections of the circles by lines indicate GCFs. The color of each circle indicates the fungal family that contains the BGC. Thus, the multiple colors linked by lines indicate GCFs that are distributed among more than one fungal family. If only a single color is present, the BGC was found only within a single family.

two different families, and only two GCFs (GCF1 and GCF3) are more widely distributed in Onygenales. These results suggest a family level specialized metabolite conservation in Onygenales.

All of the *A. pyridodomos* BGCs are singletons, except for two pathways belonging to the widely distributed GCFs 1 and 3. This result reinforces the potential family level status of this strain. We are currently working to refine this phylogenetic analysis.

We examined the three most widely occurring GCFs, GCF1–3, all of which include an NRPS gene (Figure 4). Based upon previous studies, these common GCFs are likely responsible for the production of hydroxamate siderophores, involved in iron acquisition.<sup>7</sup> For example, Hwang et al. identified GCF1 as an iron-regulated siderophore pathway (*SID1*) required for host colonization,<sup>8</sup> although the chemical structure of the siderophore was not defined. Thus, the biosynthetic pathways found in Onygenales are relatively

specific to the family level except for siderophores involved in iron acquisition.

Overall, these results indicate that Onygenales contain a mostly new and uncharacterized biosynthetic potential, at least in the PKS/NRPS gene families. Because the Onygenales include important human pathogens, characterizing this potential should be a priority.

A limitation in this study results from our current understanding of fungal biosynthesis. Fungal PKS genes are often similar, yet their chemical products differ in unpredictable ways. These differences are caused both by the PKSs and by combinations of different tailoring enzymes that modify PKS products. This reinforces the need to characterize the chemicals from Onygenales: which of the compounds are actually produced, do they contribute to pathogenesis, and do they represent new structural motifs?

**Polyketides from *A. pyridodomos*.** We grew *A. pyridodomos* for at least 1–2 months to obtain natural products and for up to a year to obtain further compounds. We selected the medium ISP2 because it was one of the few that afforded reasonable growth for this otherwise challenging isolate. While we initially worked with extracts isolated after a few weeks of fermentation, because of the slow growth of the fungus we left the culture for two months. The fungus continued to grow, and a much larger abundance of polyketides was produced. Therefore, we left the culture for a much longer period (one year) to see whether the yield would increase. To our surprise, not only did the fungus keep growing, but additional metabolites appeared after a one-year period. The new compounds appeared likely to be nonenzymatic, but interesting and novel, rearrangement products<sup>31</sup> (Table 1).

**Table 1. Compound Production after Extended Fermentation**

time	shaking/30 °C	static/21 °C
25 days	1, 3, 4, 7, 8, 9, 10, 11, 12	
60 days	1, 3, 4, 7, 8, 9, 11, 12	
365 days		1, 2, 3, 4, 5, 6, 7, 8, 9, 11, 12, 13, 14

Thus, extended fermentation may provide a method to increase chemical diversity from microbial strains. Because of the lengthy nature of this experiment, it was performed once. For this reason, it is worth attempting on other systems before generalizing our result.

In total, 14 polyketides (1–14) were isolated from *A. pyridodomos*. Our strategy was to purify all of the abundant metabolites, as Onygenales have rarely been examined

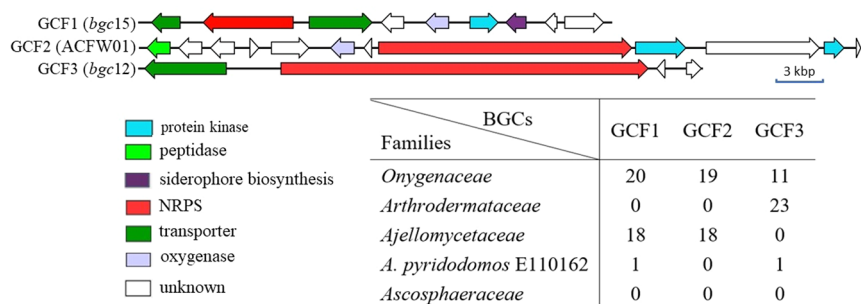


**Figure 4.** Gene organization of the most common NRPS GCFs shared among multiple families in Onygenales. GCF1 is composed of relatives of the previously identified *SID1*.<sup>8</sup>



chemically. We described five of these previously: onydecalsins A–D (**11**–**14**)<sup>21</sup> and oxazin A (**10**).<sup>20</sup> Here, we describe six further oxazin analogues (aintennols A–F (**1**–**6**)) and three other polyketides (aiorsellinates A–C (**7**–**9**)). Of these, **5**, **6**, **8**, **9**, **13**, and **14** likely represent rearrangement products (*vide infra*). The remainder of compounds represent mature products or intermediates, as experimentally defined below. Compounds **5**, **6**, **13**, and **14** were isolated only after 1 year of fermentation (Table 1).

Aintennol A (**1**) was isolated as a pale yellow solid with a molecular formula of C<sub>22</sub>H<sub>30</sub>O<sub>2</sub>. <sup>1</sup>H, <sup>13</sup>C, COSY, and HSQC NMR data (Table 2 and Figure 5) revealed that **1** has some

**Table 2.** <sup>1</sup>H (500 MHz) and <sup>13</sup>C NMR (125 MHz) Data of Compounds **1** and **2** in CDCl<sub>3</sub>

no.	<b>1</b>		<b>2</b>	
	δ <sub>C</sub> , type	δ <sub>H</sub> (J in Hz)	δ <sub>C</sub> , type	δ <sub>H</sub> (J in Hz)
1	153.0, C		159.0, C	
1-OH		7.30, brs		12.07, s
2	127.1, C		128.4, C	
3	129.8, CH	6.90, s	137.6, CH	7.17, s
4	131.7, C		130.6, C	
5	135.5, C		139.6, C	
6	123.0, C		118.2, C	
7	126.4, CH	6.40, d (15.7)	123.6, CH	6.57, d (15.7)
8	135.8, CH	6.05, dd (15.7, 10.4)	139.8, CH	6.12, dd (15.7, 10.4)
9	131.7, CH	6.22, dd (14.6, 10.8)	131.2, CH	6.28, dd (14.7, 10.8)
10	130.1, CH	5.76, dq (14.6, 6.8)	132.4, CH	5.85, dq (10.8, 6.8)
11	18.2, CH <sub>3</sub>	1.83, d (6.8)	18.6, CH <sub>3</sub>	1.85, d (6.8)
12	61.5, CH <sub>2</sub>	4.93, s	ND <sup>a</sup>	10.10, s
13	29.2, CH <sub>2</sub>	3.34, d (7.3)	31.5, CH <sub>2</sub>	3.33, d (7.3)
14	122.3, CH	5.34, t (7.3)	121.6, CH	5.31, t (7.3)
15	133.7, C		132.5, C	
16	18.1, CH <sub>3</sub>	1.76, s	17.9, CH <sub>3</sub>	1.72, s
17	26.0, CH <sub>3</sub>	1.76, s	25.7, CH <sub>3</sub>	1.76, s
18	32.4, CH <sub>2</sub>	3.21, d (7.4)	27.3, CH <sub>2</sub>	3.24, d (7.4)
19	123.6, CH	5.18, t (7.4)	122.6, CH	5.16, t (7.4)
20	131.6, C		133.4, C	
21	18.2, CH <sub>3</sub>	1.69, s	17.9, CH <sub>3</sub>	1.71, s
22	26.3, CH <sub>3</sub>	1.72, s	25.7, CH <sub>3</sub>	1.73, s

<sup>a</sup>ND = not detected.

structural features similar to those of oxazin A (**10**). A triplet olefinic proton (δ 5.34, H-14) exhibited a strong COSY correlation with a methylene group (δ 3.34, H<sub>2</sub>-13) and a weak correlation with two singlet methyl signals (δ 1.76, 6H, H<sub>3</sub>-16, 17), indicating the presence of a prenyl group in **1**. A second prenyl group in the structure can be deduced from the NMR data (δ 5.18, H-19; δ 3.21, H<sub>2</sub>-18; δ 1.69, 1.72, H<sub>3</sub>-21, 22). The COSY spectrum of **1** contained cross-peaks between H-7/H-8/H-9/H-10/H<sub>3</sub>-11, indicating that **1** has the same pentadienyl moiety as that in **10**. Additionally, five nonprotonated carbons (δ 153.0, 127.1, C-1, C-2; 131.7, 135.5, 123.0, C-3, C-4, C-5) and an aromatic methine group (δ<sub>H</sub> 6.90, δ<sub>C</sub> 129.8) were observed in the <sup>13</sup>C NMR data, revealing a pentasubstituted benzene ring. An oxygenated methylene group was observed at δ<sub>H</sub> 4.93, δ<sub>C</sub> 61.5, and an exchangeable proton signal at δ 7.30 was assigned to a phenolic hydroxy group. Finally, HMBC correlations from H<sub>2</sub>-12 to C-1, C-6, C-5, from H-7 to C-6, from H<sub>2</sub>-13 to C-1, C-2, C-3, from H<sub>2</sub>-18 to C-3,

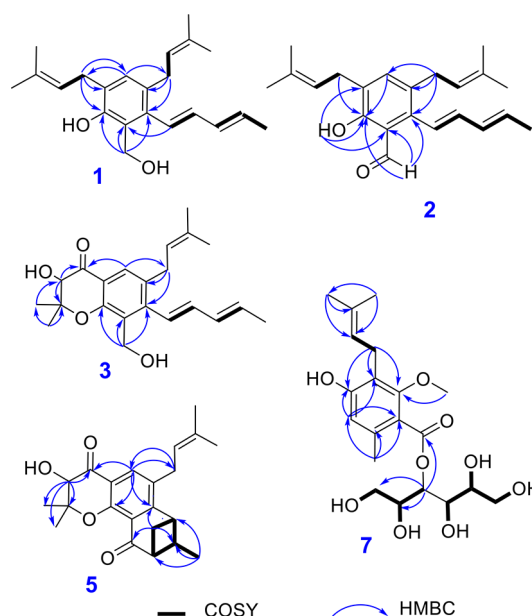


**Figure 5.** Key COSY and HMBC correlations for compounds **1**–**7**.

C-4, C-5, and from H-3 to C-13, C-18 located the substitutions of the two benzene groups, the CH<sub>2</sub>OH group, and the pentadienyl moiety on the pentasubstituted phenyl ring in **1**. The deshielded chemical shift of C-1 (δ 153.0) of the benzene ring indicated a hydroxy group at C-1, establishing the complete structure of **1**.

Aintennol B (**2**) was isolated as a yellow solid with the molecular formula C<sub>22</sub>H<sub>28</sub>O<sub>2</sub>, which is two protons lighter than **1**. This was explained by the substitution of an alcohol in **1** with an aldehyde in **2**. The <sup>1</sup>H NMR data (Table 2 and Figure 5) had very similar signals to those of **1**, except for the absence of the CH<sub>2</sub>OH group in **2**. Instead, a deshielded singlet proton was observed at δ 10.10 (H-12), consistent with an aldehyde at C-12. HMBC correlations from H-12 to C-1, C-6, and C-5 confirmed the aldehyde substitution at C-6 in the benzene ring. Further, the IR spectrum of **1** in comparison to **2** was consistent with the addition of a carbonyl. However, no HSQC correlation for H-12 was observed. Proton H-12 was not exchangeable, as overnight incubation with 10% CD<sub>3</sub>OD did not wash out the signal. Evidence for an aldehyde was further established in the deshielded shift of 1-OH (δ 7.30 brs in **1** versus δ 12.07 in **2**), resulting from a hydrogen bond between 1-OH and 12-CHO. Finally, the UV spectrum of **2** contains a λ<sub>max</sub> almost identical to that of albiducin B,<sup>32</sup> also suggesting conjugation with an aldehyde.

Aintennols C (**3**) and D (**4**) were isolated as isomeric, pale yellow solids with the molecular formula C<sub>22</sub>H<sub>28</sub>O<sub>4</sub>. The 1D NMR data (Table 3 and Figure 5) of **3** and **4** are similar to those of **1**. The major difference in comparison to **1** is that in **3** one of the isoprene groups was replaced with two singlet methyl groups (δ 1.62, 1.20, H-16, H-17), a singlet oxygenated methine group (δ<sub>H</sub> 4.40, H-3, δ<sub>C</sub> 77.4 C-3), an oxygenated nonprotonated carbon (δ<sub>C</sub> 84.4 C-2), and a ketone carbonyl (δ<sub>C</sub> 194.7, C-4). HMBC correlations from H<sub>3</sub>-16/H<sub>3</sub>-17 to C-2, C-3, from H-3 to C-2, C-4, and from H-6 to C-4 supported a 4-chromanone moiety in **3**, identical to that found in oxazin A (**10**). A spin system from H-11 to H-15 was determined to result from a pentadienyl unit based upon COSY correlations. The chemical shifts of the carbons in this pentadienyl unit are

Table 3.  $^1\text{H}$  (500 MHz) and  $^{13}\text{C}$  NMR (125 MHz) Data of Compounds 3 and 4 in  $\text{CD}_3\text{CN}$ 

no.	3		5	
	$\delta_{\text{C}}$ , type	$\delta_{\text{H}}$ (J in Hz)	$\delta_{\text{C}}$ , type	$\delta_{\text{H}}$ (J in Hz)
2	84.4, C		84.2, C	
3	77.4, CH	4.40, s	77.5, CH	4.44, s
4	194.7, C		195.1, C	
5	ND <sup>a</sup>		118.9, C	
6	125.9, CH	7.52, s	125.6, CH	7.57, s
7	134.0, C		134.1, C	
8	147.5, C		146.7, C	
9	128.8, C		126.1, C	
10	157.5, C		156.7, C	
11	126.3, CH	6.57, d (2.9)	125.0, CH	6.29, d (11.3)
12	137.8, CH	6.56, d (6.7)	133.0, CH	6.41, dd (11.9, 11.3)
13	132.5, CH	6.32, ddd (15.2, 6.7, 2.9)	128.4, CH	5.74, dd (15.0, 11.9)
14	132.9, CH	5.91, dq (15.1, 6.8)	133.5, CH	5.89, dq (15.5, 6.8)
15	18.4, CH <sub>3</sub>	1.84, d (6.8)	18.3, CH <sub>3</sub>	1.69, d (6.7)
16	26.9, CH <sub>3</sub>	1.62, s	27.1, CH <sub>3</sub>	1.62, s
17	18.0, CH <sub>3</sub>	1.20, s	18.1, CH <sub>3</sub>	1.23, s
18	32.7, CH <sub>2</sub>	3.31, m	32.3, CH <sub>2</sub>	3.22, d (6.0)
19	123.3, CH	5.20, t (6.2)	123.3, CH	5.20, t (6.2)
20	133.8, C		133.8, C	
21	17.8, CH <sub>3</sub>	1.71, s	17.8, CH <sub>3</sub>	1.66, s
22	26.0, CH <sub>3</sub>	1.74, s	26.0, CH <sub>3</sub>	1.71, s
23	56.6 CH <sub>2</sub>	4.61 d (11.7), 4.55 d (11.7)	57.3, CH <sub>2</sub>	4.53, brs

<sup>a</sup>ND = not detected.

very similar to those found in oxazin A, indicating the same *trans* double bonds in **3**, while the chemical shifts of the protons are very different. (This difference is caused by deshielding from an adjacent aromatic group in **10**.) Because of overlap between H-11 and H-12, a HOMODEC decoupling experiment (Figure S56) helped to improve coupling constant accuracy. An unusually small coupling constant was observed between H-12 and H-13 ( $J_{\text{H12-H13}} = 6.7$  Hz). The 1D NMR data of **4** differed from those of **3** only in the chemical shifts and *J*-values of the pentadienyl unit, especially for positions 11, 12, and 13 (Table 3). The coupling constant ( $J_{\text{H11-H12}} = 11.3$  Hz) suggested a *cis* configuration of the C-11/C-12 double bond in **4**. There was no observed Cotton effect in the electronic circular dichroism (ECD) spectrum of **3** and **4**, despite a strong dynode voltage corresponding to the UV absorption spectra. Thus, as found for **10**, **3** and **4** are racemic.

Aintennols E (**5**) and F (**6**) were isolated only after 1 year of fermentation as isomeric, pale yellow solids with the molecular formula  $\text{C}_{22}\text{H}_{26}\text{O}_4$ . The 1D NMR data (Table 4 and Figure 5) of **5** and **6** are almost identical. The spectra for **5** and **6** were similar to those for **3** and **4**, with most differences at C-23 and C-11–C-15. A ketone carbonyl ( $\delta_{\text{C}}$  198.1, C-23), three methines ( $\delta_{\text{C}}$  40.5, C-11, 46.9, C-12, 54.7, C-13), a methylene ( $\delta_{\text{C}}$  38.2, C-14), and a doublet methyl ( $\delta_{\text{C}}$  12.7, C-15) were observed in the 1D NMR data of **5**. COSY correlations between H-11/H-12/H-13/H<sub>2</sub>-14/H<sub>3</sub>-15 suggested that all of the protons for the additional  $\text{sp}^3$  carbons are in a single spin system. HMBC correlations from H<sub>3</sub>-15 to C-11, C-12, C-13 and from H<sub>2</sub>-14 to C-12 and C-23 established a benzobicyclo[3.1.1]heptanone moiety in the structure of **5**. HMBC correlations from H-14 to C-8 supported the link

Table 4.  $^1\text{H}$  (500 MHz) and  $^{13}\text{C}$  NMR (125 MHz) Data of Compounds 5 and 6 in  $\text{CD}_3\text{CN}$ 

no.	5		6	
	$\delta_{\text{C}}$ , type	$\delta_{\text{H}}$ (J in Hz)	$\delta_{\text{C}}$ , type	$\delta_{\text{H}}$ (J in Hz)
2	83.6, C		83.9, C	
3	76.1, CH	4.49, s	76.2, CH	4.46, s
4	193.6, C		193.3, C	
5	ND <sup>a</sup>		ND <sup>a</sup>	
6	131.1, CH	7.77, s	131.0, CH	7.78, s
7	ND <sup>a</sup>		ND <sup>a</sup>	
8	156.2, C		156.0, C	
9	ND <sup>a</sup>		ND <sup>a</sup>	
10	157.4, C		157.0, C	
11	40.5, CH	3.60, q (5.8)	40.8, CH	3.60, q (5.8)
12	46.9, CH	3.20, m	46.4, CH	3.19, m
13	54.7, CH	3.07, q (5.5)	55.7, CH	3.07, q (5.5)
14	38.2, CH <sub>2</sub>	2.59, dq (9.4, 5.8); 2.17, d (9.4)	38.5, CH	2.59, dq (9.4, 5.8); 2.17, d (9.4)
15	12.7, CH <sub>3</sub>	0.83, d (7.0)	12.2, CH <sub>3</sub>	0.79, d (6.7)
16	26.4, CH <sub>3</sub>	1.76, s	26.1, CH <sub>3</sub>	1.76, s
17	17.0, CH <sub>3</sub>	1.24, s	16.8, CH <sub>3</sub>	1.26, s
18	30.7, CH <sub>2</sub>	3.27, m	30.8, CH <sub>2</sub>	3.27, m
19	121.3, CH	5.05, t (6.2)	121.6, CH	5.06, t (6.2)
20	132.8, C		133.1, C	
21	17.7, CH <sub>3</sub>	1.70, s	17.2, CH <sub>3</sub>	1.70, s
22	25.3, CH <sub>3</sub>	1.71, s	25.4, CH <sub>3</sub>	1.71, s
23	198.1, C		197.3, C	

<sup>a</sup>ND = not detected.

between the benzobicyclo[3.1.1]heptanone moiety and the prenylated benzene ring. The chemical shifts and coupling constants for H-14 in both **5** and **6** are almost identical to those of a synthetic compound, *endo*-2-isopropyl-2,3-dihydro-1,3-methanonaphthalen-4(1*H*)-one, but drastically different from *exo*-2-isopropyl-2,3-dihydro-1,3-methanonaphthalen-4(1*H*)-one.<sup>33</sup> This finding established an *endo*-benzobicyclo[3.1.1]heptanone moiety in **5** and **6**. There was no observed Cotton effect in the ECD spectra of **5** and **6**, indicating that both are racemic. The  $^1\text{H}$  NMR and  $^{13}\text{C}$  spectra of **5** and **6** are almost identical, with only slight differences between them. In extended incubation in methanol, **5** and **6** slowly interconvert, indicating that the difference between the compounds is at a labile center and not at the carbocycle. Because C-3 is racemic in compounds **3** and **4** and the C-3 position is labile due to the adjacent carbonyl, it is likely that **5** and **6** differ in the relative orientation between C-3 and the carbocyclic portion. The absence of a Cotton effect in **5** and **6** indicates that the carbocycle is also racemic. This indicates that the formation of the benzobicyclo[3.1.1]heptanone moiety in **5** and **6** is likely nonenzymatic. Thus, **5** and **6** are both racemic; they are diastereomers that differ by the relative configuration between C-3 and the *endo*-benzobicyclo[3.1.1]heptanone moiety. The absence of distance correlations between the two halves of the molecules precluded establishment of the relative configurations of **5** and **6**.

Aiorsellinate (**7**) was isolated as a colorless oil with the molecular formula  $\text{C}_{20}\text{H}_{30}\text{O}_9$ . The presence of a benzene ring in **7** was deduced by the interpretation of HMBC and COSY correlations (Figure 5). The six aromatic carbons, including a methine (C-6,  $\delta$  112.6) and five nonprotonated carbons (C-2–5,  $\delta$  120.9, 157.0, 119.3, 157.7 and C-7  $\delta$  135.0), indicated the presence of a highly substituted doubly oxygenated benzene

Table 5.  $^1\text{H}$  (500 MHz) and  $^{13}\text{C}$  NMR (125 MHz) Data of Compounds 7–9 in  $\text{DMSO}-d_6$ 

no.	7		8		9	
	$\delta_{\text{C}}$ , type	$\delta_{\text{H}}$ (J in Hz)	$\delta_{\text{C}}$ , type	$\delta_{\text{H}}$ (J in Hz)	$\delta_{\text{C}}$ , type	$\delta_{\text{H}}$ (J in Hz)
1	168.7, C		167.2, C		167.7, C	
2	120.9, C		119.8, C		119.1, C	
3	157.0, C		156.3, C		155.9, C	
4	119.3, C		118.4, C		118.0, C	
5	157.7, C		156.9, C		156.5, C	
6	112.6, CH	6.50, s	112.0, CH	6.43, s	111.7, CH	6.44, s
7	135.0, C		134.2, C		133.7, C	
8	20.1, $\text{CH}_3$	2.19, s	20.6, $\text{CH}_3$	2.14, s	19.6, $\text{CH}_3$	2.12, s
9	23.0, $\text{CH}_2$	3.22 d, (6.8)	22.4, $\text{CH}_2$	3.15, d (6.7)	22.2, $\text{CH}_2$	3.16, d (6.7)
10	123.1, CH	5.16, t (6.8)	123.0, CH	5.10, t (6.5)	122.4, CH	5.11, t (6.7)
11	131.3, C		130.1, C		129.7, C	
12	26.2, $\text{CH}_3$	1.62, s	24.9, $\text{CH}_3$	1.60, s	25.3, $\text{CH}_3$	1.60, s
13	18.2, $\text{CH}_3$	1.74, s	15.1, $\text{CH}_3$	1.68, s	17.0, $\text{CH}_3$	1.68, s
14	62.7, $\text{CH}_3$	3.69, s	62.8, $\text{CH}_3$	3.63, s	61.8, $\text{CH}_3$	3.64, s
1'	64.0, $\text{CH}_2$ (64.3) <sup>a</sup>	3.65, m; 3.44, m	60.5, $\text{CH}_2$	3.81, m; 3.66, m	67.6, $\text{CH}_2$	4.48, d (11.3); 4.11, dd (11.3, 6.9)
1'-OH		4.39, t (5.2)		4.59, t (5.0)		
2'	71.3, CH (71.2) <sup>a</sup>	3.87, m	75.2, CH	5.02, m	68.3, CH	3.74, dd (8.0, 7.0)
2'-OH		5.00, d (5.3)				
3'	73.5, CH (73.8) <sup>a</sup>	5.27, d (7.4)	67.5, CH	3.97, dd (7.5, 7.5)	71.0, CH	3.45, m
3'-OH				4.52, d (7.5)		
4'	71.0, CH (71.1) <sup>a</sup>	3.42, m	70.9, CH	3.45, m	69.4, CH	3.59, m
4'-OH		4.35, d (5.7)		4.47, d (5.2)		
5'	69.7, CH (69.7) <sup>a</sup>	3.85, m	70.9, CH	3.36, m	69.2, CH	3.56, m
5'-OH		4.74, d (5.2)		4.22, d (8.0)		
6'	63.5, $\text{CH}_2$ (63.8) <sup>a</sup>	3.63, m; 3.43, m	63.7, $\text{CH}_2$	3.60, m; 3.36, m	63.6, $\text{CH}_2$	3.59, m; 3.37, m
6'-OH		4.58, t (5.0)		4.34, t (5.6)		

<sup>a</sup> $^{13}\text{C}$  chemical shifts (obtained from HSQC spectrum) in compound 7a.

ring in the structure of 7. The HMBC correlations from  $\text{H}_2$ -9 to C-3, C-4, and C-5 established the prenyl group at C-4. The HMBC correlations from  $\text{H}_3$ -8 to C-2, C-6, and C-7, from H-6 to C-2, C-4, and C-5, and from  $\text{H}_3$ -14 to C-3, as well as the chemical shifts of C-3 and C-5 established the placement of the other groups on the benzene ring. The chemical shift of C-2 and the ester carbonyl at C-1 determined the position of the ester and established the presence of a prenylated orsellinate moiety. The remaining six oxygenated  $\text{sp}^3$ -hybridized carbons and five alcohol exchangeable protons (Table 5) suggested a hexitol moiety, which was confirmed by COSY correlations between H-1'/H-2'/H-3' and between H-6'/H-5'/H-6'. Finally, the HMBC correlation from H-3' to C-1 established an ester bond between the orsellinate moiety and hexitol moiety. To further confirm the structure, 7 was hydrolyzed and analyzed by LC-MS. A new product ( $m/z$  251  $[\text{M} + \text{H}]^+$ ) was observed, which corresponded to the expected carboxylate of 7 (Figure S5). Mass spectrometric fragmentation data of 7 provided further evidence for the structure (Figure S6). In particular, an ion at  $m/z$  233 suggested a loss of a hexitol (182 Da) in comparison to an ion at  $m/z$  415 ( $[\text{M} + \text{H}]^+$ ), while the ion at  $m/z$  251 suggested an addition of  $\text{H}_2\text{O}$  to the ion at  $m/z$  233. An ion at  $m/z$  195, which is 56 Da less than the ion at  $m/z$  251, suggested a loss of  $\text{C}_4\text{H}_8$  from the prenyl group.

Aiorsellinates B (8) and C (9) were constitutional isomers of 7. The NMR data of 8 and 9 were very similar to those of 7

except for the chemical shifts of the hexitol moiety. In comparison to 7, the chemical shifts of protons and carbon at C-1' ( $\delta_{\text{H}}$  4.48, 4.11,  $\delta_{\text{C}}$  67.6) in 8 were deshielded, while in 9 those at C-2' ( $\delta_{\text{H}}$  5.02,  $\delta_{\text{C}}$  75.2) were deshielded. This suggested ester bond migration to C-2' in 8 and to C-1' in 9, respectively. Indeed, treatment of 7 in  $\text{Na}_2\text{CO}_3$  solution overnight led to an accumulation of 8 and 9. In early time points of the fungal fermentation (10 days), only 7 was present, while at later points 8 and 9 accumulated. Because 7 was the major component in the extract of the fungus at all time points, 7 is the likely enzymatic product of the pathway.

Coupling constants indicated that the hexitols in 7–9 were likely to be either sorbitol or mannitol. Chemical shifts of the hexitols in 7–9 matched those of mannitol very well, especially C-2' to C-6' of 7, which were almost identical to the same carbons found in mannitol. Analogue 7a was synthesized and had nearly identical chemical shifts and coupling constants to those of 7, supporting the presence of mannitol. By comparing the experimental and calculated ECD spectra (Figure S7) of 7, the hexitol was determined to be D-mannitol.

#### Biological Activities of *A. pyridodomos* Polyketides.

Several of the new compounds were active in assays. We first investigated the extract because it showed activity against a panel of transient receptor potential channels. TRPs are important throughout the body and include several channels important in itch and pain, which may potentially be of interest

in topical fungal infections.<sup>3,4</sup> However, the purified compounds were only modestly active. In particular, **1** was active against TRPV3 and TRPV4 at 32 and 70  $\mu\text{M}$ , respectively. The compounds were tested for activity against *Histoplasma capsulatum*. Several compounds exhibited modest activity (Table 6), with selectivity for *H. capsulatum* in comparison to other fungi.

**Table 6. Anti-*Histoplasma* Activity of Purified Compounds**

compound	<i>Histoplasma</i> IC <sub>50</sub> ( $\mu\text{g/mL}$ )
<b>1</b>	8
<b>3</b>	16
<b>5</b>	32
<b>6</b>	64
<b>13</b> <sup>a</sup>	2
<b>14</b> <sup>a</sup>	16
amphotericin B	0.5
itraconazole	0.001

<sup>a</sup>Previously reported data.<sup>21</sup>

**Identification of Biosynthetic Gene Clusters.** Biogenetic hypotheses for **1**–**14** were proposed based upon structural data. Compounds **1**–**14** are all polyketide derivatives that are likely to result from one of the 14 PKS genes in the genome. Aintennols (**1**–**6**) and oxazinin (**10**) likely result from a single biosynthetic pathway, in which **1** or **3** is the probable primary enzymatic product. This pathway would require at least one prenyltransferase, at least one oxidase, and at least one PKS with a terminal reduction domain. Indeed, one BGC was identified to have all of these features, which were absent in other clusters in the genome; this cluster was

named “ain” for its putative role in biosynthesis of **1** (Figure S4). Onydecalsins (**11**–**14**) were previously defined as biogenetically similar to betaenones,<sup>35</sup> the biosynthesis of which has been well defined by the Oikawa group;<sup>36</sup> a single betaenone-like cluster (*ond*) is present in the genome (Figure S8). Work is ongoing in our laboratories to biochemically confirm this assignment.

Finally, aiorsellinates (**7**–**9**) originate with the single compound **7**. In this instance, the core structure appears to be composed of orsellinic acid, the biosynthesis of which has been well studied for decades,<sup>37</sup> while new decorations of O-methylation, prenylation, and esterification make the compound unique. A single BGC, *aio* (Figure 6), contained putative orsellinate PKS (AioS), prenyltransferase (AioP), methyltransferase (AioM), and possible mannitol transferase (AioT) genes. Predicted AioS is very similar to characterized orsellinic acid synthases, except that it terminates with an acyl carrier protein domain instead of a thioesterase. We propose that the neighboring AioT is likely to be involved in the transfer of the ACP-linked orsellinate group, in analogy to a similar protein involved in trichothecene species acetylation. Other alternatives include the possibility that mannitol could be added as a detoxification mechanism, which may not be encoded by AioT.

To confirm these assignments, we turned to heterologous expression in a model fungus. This route was chosen because of the challenge of generating a new genetic model,<sup>38</sup> especially because we have not yet found conditions under which sporulation occurs for this new family. Genes *aioS*, *aioM*, *aioP*, and *aioT* were cloned into an expression vector that we designed for high-titer polyketide expression and then transformed either singly or in combination into the expression

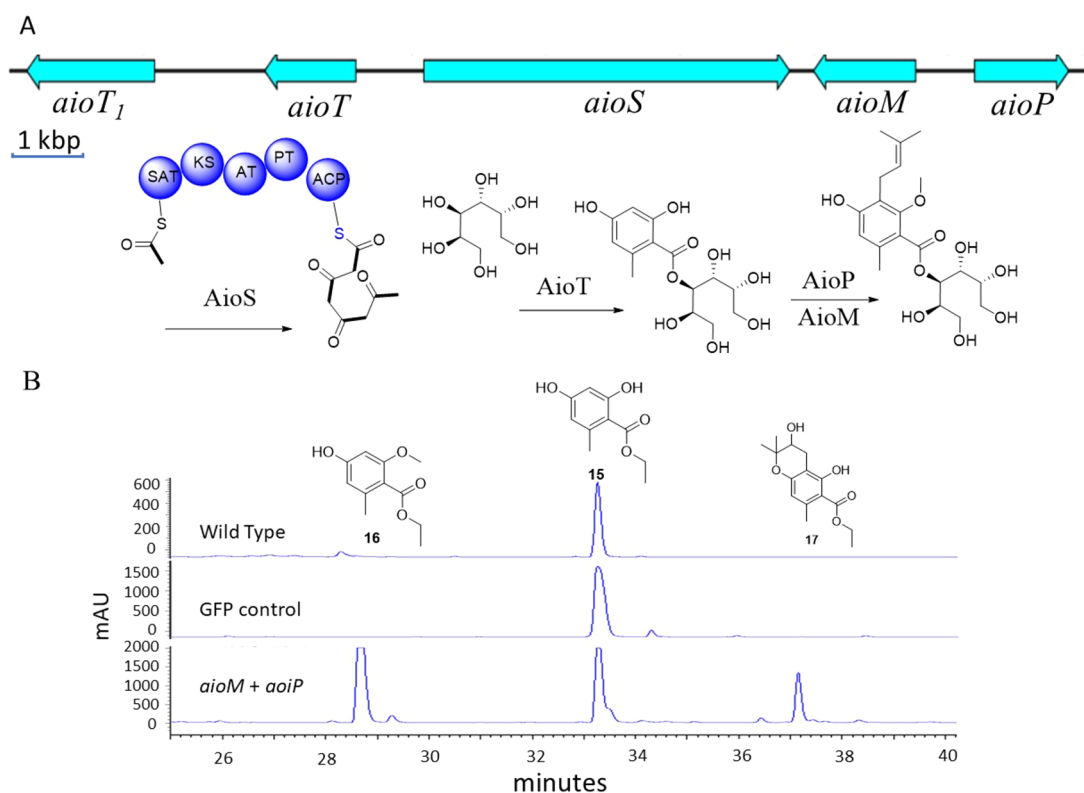


**Figure 6.** (A) *aio* gene cluster and domain organization of the PKS gene. (B) The genes *aioT*, *aioS*, *aioM*, and *aioP* were overexpressed in *F. heterosporum*. Incubation with precursor analogue **15** led to formation of two new compounds (**16** and **17**), as shown in HPLC traces at 290 nm.



host, *Fusarium heterosporum*.<sup>39</sup> In some cases, we have detected >1 g/kg of heterologous polyketides using this strategy. However, in this instance no new products could be detected. We reasoned that the likely limiting factor would be the PKS, as occasionally these genes do not adapt well to heterologous systems. Therefore, we added orsellinate ethyl ester to the medium (for better cell penetration in comparison to the free acid), affording the predicted prenylated and methylated products only when the correct genes were in place (Figure 6). These derivatives were further modified by oxidation of the isoprene group in the course of fermentation by a nonspecific oxidase in the *F. heterosporum* genome, indicating that *F. heterosporum* may not be a good host for heterologous production of 1–3. By contrast, in control fermentations consisting of wild-type *F. heterosporum* or a mutant containing GFP in place of *aiO* genes, no new products were detected unless orsellinic acid ethyl ester was supplied. This demonstrates that *aiOP* and *aiOM* are the functional orsellinate prenyltransferase and methyltransferase, respectively.

## CONCLUSION

We describe 14 natural products that are so far unique to a new family of Onygenales fungi represented by *A. pyridodoms*. We tentatively assigned their BGCs and confirmed one of the assignments by heterologous expression. A large number of uncharacterized natural products and BGCs await analysis in the order Onygenales, which is a key group of pathogenic fungi.

## EXPERIMENTAL SECTION

**General Experimental Procedures.** Circular dichroism spectra were obtained on a Jasco J720A spectropolarograph. IR spectra were measured on a Thermo Fisher iS50 Fourier transform IR spectrometer. NMR data were collected using either a Varian INOVA 500 (<sup>1</sup>H 500 MHz, <sup>13</sup>C 126 MHz) NMR spectrometer with a 3 mm Nalorac MDBG probe or a Varian INOVA 600 (<sup>1</sup>H 600 MHz, <sup>13</sup>C 150 MHz) NMR spectrometer equipped with a 5 mm [<sup>1</sup>H/<sup>13</sup>C, <sup>15</sup>N] triple resonance cold probe with a z-axis gradient, utilizing residual solvent signals for referencing.<sup>40</sup> High-resolution mass spectra (HRMS) were obtained using a Bruker APEXII FTICR mass spectrometer equipped with an actively shielded 9.4 T superconducting magnet (MagneX Scientific Ltd.), an external Bruker APOLLO ESI source, and a Synrad S0W CO<sub>2</sub> CW laser. Supelco Discover HS (4.6 × 150 mm) and semipreparative (10 × 150 mm) C18 (5 μm) columns were used for analytical and semipreparative HPLC, respectively, as conducted on a Hitachi Elite Lachrom System equipped with a diode array L-2455 detector. Unless stated otherwise, all reagents and solvents were purchased from commercial suppliers, and all reactions were carried out under anhydrous conditions with an argon atmosphere. Yields were calculated by HPLC chromatography or <sup>1</sup>H NMR spectroscopy.

**Fermentation and Extraction.** *A. pyridodoms* strain was grown and extracted as previously described.<sup>21</sup>

**Purification.** The extract B<sup>21</sup> (600 mg) from a 1-year-old culture was separated into seven fractions (Fr1–Fr7) on a C<sub>18</sub> column using step-gradient elution of MeOH in H<sub>2</sub>O (20%, 40%, 60%, 70%, 80%, 90%, and 100%). Fr3 was further subjected to C<sub>18</sub> HPLC (35% CH<sub>3</sub>CN in H<sub>2</sub>O) to yield compounds 7 (2.5 mg), 8 (1.0 mg), and 9 (1.1 mg). Fr6 was purified by C<sub>18</sub> HPLC (85% CH<sub>3</sub>CN in H<sub>2</sub>O) to yield compound 1 (4.2 mg). Fr7 was purified by C<sub>18</sub> HPLC (89% CH<sub>3</sub>CN in H<sub>2</sub>O) to yield compound 2 (1.0 mg). Fr5 was fractionated using a gradient HPLC method (50% CH<sub>3</sub>CN in H<sub>2</sub>O to 80% CH<sub>3</sub>CN in H<sub>2</sub>O over 20 min) to yield five subfractions (Fr5-1–Fr5-5). Fr5-3 was purified by C<sub>18</sub> HPLC (63% CH<sub>3</sub>CN in H<sub>2</sub>O) to yield compound 3 (8.0 mg) and 4 (7.0 mg). Fr5-4 was purified by C<sub>18</sub> HPLC (66% CH<sub>3</sub>CN in H<sub>2</sub>O) to yield compounds 5 (1.0 mg) and 6

(1.2 mg). Compounds 1, 3, 4, 7, 8, and 9 were also isolated from a 2-month shaking culture (extracts A)<sup>21</sup> following a similar separation procedure.

**Aintennol A (1):** pale yellow solid; UV (MeOH) λ<sub>max</sub> 224, 267 nm; IR (polyethylene) ν<sub>max</sub> 3501, 2972, 1452, 1249, 1230, 1000 cm<sup>-1</sup>; <sup>1</sup>H and <sup>13</sup>C NMR (Table 2); HRESIMS *m/z* 325.2167 [M – H]<sup>–</sup> (calcd for C<sub>22</sub>H<sub>30</sub>O<sub>2</sub>, 325.2168).

**Aintennol B (2):** yellow solid; UV (MeOH) λ<sub>max</sub> 250, 285, 371 nm; IR (polyethylene) ν<sub>max</sub> 2960, 1692, 1641, 1450, 1301, 1261, 991, 770 cm<sup>-1</sup>; <sup>1</sup>H and <sup>13</sup>C NMR (Table 2); HRESIMS *m/z* 325.2166 [M + H]<sup>+</sup> (calcd for C<sub>22</sub>H<sub>28</sub>O<sub>2</sub>, 325.2168).

**Aintennol C (3):** pale yellow solid; UV (MeOH) λ<sub>max</sub> 229, 308, 350 nm; IR (polyethylene) ν<sub>max</sub> 3422, 2981, 1692, 1611, 1440, 1260, 1103 cm<sup>-1</sup>; <sup>1</sup>H and <sup>13</sup>C NMR (Table 3); HRESIMS *m/z* 357.2066 [M + H]<sup>+</sup> (calcd for C<sub>22</sub>H<sub>28</sub>O<sub>4</sub>, 357.2066).

**Aintennol D (4):** pale yellow solid; UV (MeOH) λ<sub>max</sub> 228, 265, 297, 343 nm; IR (polyethylene) ν<sub>max</sub> 3421, 2982, 1692, 1602, 1433, 1261, 1104 cm<sup>-1</sup>; <sup>1</sup>H and <sup>13</sup>C NMR (Table 3); HRESIMS *m/z* 357.2067 [M + H]<sup>+</sup> (calcd for C<sub>22</sub>H<sub>28</sub>O<sub>4</sub>, 357.2066).

**Aintennol E (5):** yellow solid; UV (MeOH) λ<sub>max</sub> 205, 242, 266, 354 nm; IR (polyethylene) ν<sub>max</sub> 2972, 1691, 1600, 1454, 1212, 1110 cm<sup>-1</sup>; <sup>1</sup>H and <sup>13</sup>C NMR (Table 4); HRESIMS *m/z* 355.1907 [M + H]<sup>+</sup> (calcd for C<sub>22</sub>H<sub>26</sub>O<sub>4</sub>, 355.1909).

**Aintennol F (6):** yellow solid; UV (MeOH) λ<sub>max</sub> 205, 242, 266, 354 nm; IR (polyethylene) ν<sub>max</sub> 2972, 1700, 1600, 1453, 1212, 1111 cm<sup>-1</sup>; <sup>1</sup>H and <sup>13</sup>C NMR (Table 4); HRESIMS *m/z* 355.1908 [M + H]<sup>+</sup> (calcd for C<sub>22</sub>H<sub>26</sub>O<sub>4</sub>, 355.1909).

**Aiorsellinate A (7):** pale yellow solid; UV (MeOH) λ<sub>max</sub> 199, 251 nm; ECD (0.5 mg/mL, methanol), λ<sub>max</sub> (Δε) 290 (–0.8), 254 (1.23) nm; IR (polyethylene) ν<sub>max</sub> 3390, 1712, 1598, 1463, 1272, 1080 cm<sup>-1</sup>; <sup>1</sup>H and <sup>13</sup>C NMR (Table 5); HRESIMS *m/z* 415.1969 [M + H]<sup>+</sup> (calcd for C<sub>20</sub>H<sub>30</sub>O<sub>9</sub>, 415.1963).

**Aiorsellinate B (8):** pale yellow solid; UV (MeOH) λ<sub>max</sub> 199, 251 nm; IR (polyethylene) ν<sub>max</sub> 3391, 1712, 1598, 1462, 1272, 1081 cm<sup>-1</sup>; <sup>1</sup>H and <sup>13</sup>C NMR (Table 5); HRESIMS *m/z* 415.1970 [M + H]<sup>+</sup> (calcd for C<sub>20</sub>H<sub>30</sub>O<sub>9</sub>, 415.1963).

**Aiorsellinate C (9):** pale yellow solid; UV (MeOH) λ<sub>max</sub> 199, 251 nm; IR (polyethylene) ν<sub>max</sub> 3390, 1712, 1599, 1461, 1272, 1082 cm<sup>-1</sup>; <sup>1</sup>H and <sup>13</sup>C NMR (Table 5); HRESIMS *m/z* 415.1969 [M + H]<sup>+</sup> (calcd for C<sub>20</sub>H<sub>30</sub>O<sub>9</sub>, 415.1963).

**Sequencing.** The mycelium of *A. pyridodoms* was collected by centrifugation and then extracted as previously described.<sup>41</sup> The resulting DNA samples were repurified with the Genomic DNA Clean & Concentrator kit (Zymo Research). Illumina libraries were prepared as ~350 bp inserts from genome DNA. Libraries were sequenced using an Illumina HiSeq 2000 sequencer in 101 bp/125 bp paired-end runs. Raw fasta files were trimmed by sickle and assembled using IDBA\_ud<sup>42</sup> (--mink = 20 --maxk = 100 --step = 20 --inner\_mink = 10 --inner\_step = 5 --prefix = 3 --min\_count = 2 --min\_support = 1 --num\_threads = 0 ==seed\_kmer = 30 --min\_contig = 200 --similar = 0.95 --max\_mismatch = 3 --min\_pairs = 3). The genome was annotated using Augustus<sup>43</sup> de novo gene prediction parameters, with ‘Coccidioides immitis’ as the model organism. The resulting gff output file was converted to a GenBank file and submitted to the RAST<sup>44–46</sup> online server for gene identification.

**GCF Analysis.** The Augustus<sup>43</sup> annotation output was converted to a GenBank file and used as the input for a standalone version of antiSMASH 4.0.<sup>22</sup> All BGCs were separated into individual GenBank files. Initial pairwise similarity matrices between every BGC pair were calculated using MultiGeneBlast<sup>28</sup> with the parameters (–distancekb 10 –minperc 50 –minseqcov 80) and then normalized as follows: (1) The “total score” (MultiGeneBlast) between the query BGC and itself was set as 1.0; (2) the “total score” between query BGC and target BGC was normalized to the total score between query itself in step 1. BGC pairs with a final pairwise similarity matrix (normalized score) over 0.6 were selected and visualized in Cytoscape.<sup>30</sup> Each GCF was manually checked by examining the MultiGeneBlast alignment.

**Construction of Phylogenetic Tree.** Proteins encoded in Onygenales genomes were obtained using the Augustus annotation output. Seventeen widespread genes present in a single copy in all genomes were identified by performing a blastp search using *A. pyridodomo*s against 68 other Onygenales genomes. Hits were defined as identity > 80%, query coverage > 0.8, and subject coverage > 0.8. Genes that met those criteria and that were present in all 68 Onygenales genomes were selected and used for phylogenetic analysis. Orthologous genes were aligned using t-Coffee<sup>47</sup> (-mode mcoffee -output = msf, fasta\_aln). To remove poorly aligned regions, the resulting alignment was subsequently trimmed with trimAl v1.4<sup>48</sup> with a gap threshold of 0.4. A concatenation of alignment of all conserved proteins was done by PerlScript catfasta2phyml.pl (<https://github.com/nylander/catfasta2phyml>). The maximum likelihood trees were constructed using MEGA-X using the Jukes–Cantor model and 500 bootstrap replicates to assess node support.

**Bioactivity Screening.** Assays were performed as previously described.<sup>21</sup>

**Synthesis of Compound 7a.** (See Scheme S1.) Ethyl orsellinate (P1) was prepared as reported by Chen et al.<sup>49</sup> Ethyl 4-(benzyloxy)-2-hydroxy-6-methylbenzoate (P3) was prepared as described by Zhu et al.<sup>50</sup> Product P3 (300 mg) was treated with LiOH (96 mg) in MeOH–H<sub>2</sub>O (1:2; 10 mL). The solution was refluxed for 5 h to yield product P4 (270 mg). A mixture of product P4 (260 mg), thionyl chloride (2 mL), and dimethylformamide (DMF) (100  $\mu$ L) in dry CH<sub>2</sub>Cl<sub>2</sub> (150 mL) was heated to reflux for 6 h, and then the extra thionyl chloride was removed under vacuum to yield product P5 (290 mg, oil). 1,2:5,6-Bis-O-(1-methylethylidene)-D-mannitol (262 mg) in tetrahydrofuran (THF) (100 mL) was pretreated with NaH (40 mg, 60% in mineral oil) for 1 h and added to the flask containing product P5 (210 mg). The resulting mixture was stirred for 2 h to yield product P6 (350 mg). Product P6 (300 mg) was dissolved in 100 mL of EtOH, 10% palladium on carbon (30 mg) was added, and the mixture was treated with hydrogen gas (1 atm) for 3 h to yield product P7 (200 mg). Product P7 (42 mg) was dissolved in dry DMF (50 mL), and NaH (4 mg, 60% in mineral oil) was added. The mixture was stirred at 40 °C for 2 h and cooled to room temperature. 3,3-Dimethylallyl bromide (14.7 mg, 12  $\mu$ L) was added, and the mixture was stirred at 60 °C overnight. The product was precipitated by adding H<sub>2</sub>O (100 mL), filtered, and washed with H<sub>2</sub>O to yield a white solid, which was further treated with 6 M HCl (10 mL) and purified by C18 HPLC (20% MeCN in H<sub>2</sub>O) to yield compound 7a (2.1 mg): <sup>1</sup>H NMR (600 MHz, DMSO-*d*<sub>6</sub>)  $\delta$ <sub>H</sub> 9.59 (1H, s, 5-OH); 6.34 (1H, s, H-6); 5.16 (1H, d, *J* = 7.6 Hz, H-3'); 4.95 (1H, t, H-10); 4.83 (1H, d, 2'-OH); 4.57 (1H, d, 5'-OH); 4.43 (1H, t, 6'-OH); 4.30 (1H, t, 1'-OH); 4.22 (1H, d, 4'-OH); 3.75 (1H, m, H-2'); 3.75 (1H, m, H-5'); 3.38 (1H, m, H-4'); 3.63 (3H, s, H-14); 3.62 (1H, m, H-1'a); 3.33 (1H, m, H-1'b); 3.59 (1H, m, H-6'a); 3.38 (1H, m, H-6'b); 3.17 (2H, d, H-9); 2.06 (3H, s, H-8); 1.55 (1H, m, H-11); 1.69 (3H, s, H-12); 1.61 (3H, s, H-13); ESIMS *m/z* 415 [M + H]<sup>+</sup>.

**Heterologous Expression and Biosynthesis.** See Table S1 for primer sequences. *pyrG-aioS+aiOT*: the *pks* gene (*aioS*) was amplified by PCR in two pieces from genomic DNA with primer pairs 160PKS\_PyrG\_Fwd/in\_160PKS\_pyrG\_Rev and in\_160PKS\_PyrG\_Fwd/160PKS\_pyrG\_Rev. The resulting fragments were cloned into NotI-linearized *pPyrG517-deg3ER\_plus\_sgfp* by yeast recombination to afford *pyrG-aioS+gfp* plasmid. The acyltransferase gene (*aiOT*) was amplified with primer pair 160Trs\_pyrG\_Fwd/160Trs\_pyrG\_Rev and transformed into *S. cerevisiae* BY4741 together with *PmeI*-cut *pyrG-aioS+gfp* for recombination to make the final plasmid. *pHyg-aiOM+aiOP*: The methyltransferase gene (*aiOM*) was amplified with primer pair 160MT-Fwd/160MT-Rev. The prenyltransferase (*aiOP*) was amplified with primer pair 160prenyl-Fwd/160prenyl-Rev. Both amplicons were cloned into NotI- and *PmeI*-cut overexpression vector FH-3 by yeast recombination.

*F. heterosporum* was transformed with plasmids using previously reported methods.<sup>39</sup> The transformed mutant strain carrying the four genes (*aioS+aiOT+aiOM+aiOP*) was cultured in potato dextrose broth (150 mL) at 30 °C with shaking at 180 rpm for 14 days. Sterile-filtered compound 15 (20 mg in 0.2 mL of MeOH) was added at the

72 h time point of the culture. The culture was harvested and extracted with EtOAc. The products were analyzed by HPLC-DAD, LC-MS, and NMR, resulting in the identification of two new compounds, 16 and 17. Compound 16: <sup>1</sup>H NMR (500 MHz, CDCl<sub>3</sub>)  $\delta$ <sub>H</sub> 6.27 (1H, s); 6.24 (1H, s); 4.36 (2H, q, *J* = 7.1 Hz); 3.78 (3H, s); 2.25 (3H, s); 1.36 (3H, t, *J* = 7.1 Hz); ESIMS *m/z* 211 [M + H]<sup>+</sup>. Compound 17: <sup>1</sup>H NMR (500 MHz, CDCl<sub>3</sub>)  $\delta$ <sub>H</sub> 11.87 (1H, s); 6.28 (1H, s); 4.64 (1H, t, *J* = 8.8 Hz); 4.40 (2H, q, *J* = 7.1 Hz); 3.04 (2H, m); 2.43 (3H, s); 1.43 (3H, t, *J* = 7.1 Hz); 1.36 (3H, s); 1.23 (3H, s); ESIMS *m/z* 281 [M + H]<sup>+</sup>.

**ECD Calculation.** ECD calculation was performed as previously described.<sup>21</sup>

## ■ ASSOCIATED CONTENT

### Supporting Information

The Supporting Information is available free of charge on the ACS Publications website at DOI: 10.1021/acs.jnatprod.9b00121.

Additional information (PDF)

## ■ AUTHOR INFORMATION

### Corresponding Author

\*Tel: 801-585-5234. Fax: 801-581-7087. E-mail: [ews1@utah.edu](mailto:ews1@utah.edu).

### ORCID

Christopher A. Reilly: 0000-0002-5006-1982

Eric W. Schmidt: 0000-0001-5839-694X

### Notes

The authors declare no competing financial interest.

## ■ ACKNOWLEDGMENTS

This work was funded by NIH R01GM107557 and R35GM122521 to E.W.S. and C.R. and NIH R00AI112691 and R01AI137418 to S.B. We thank the University of Utah Center for High Performance Computing for access to computational resources.

## ■ REFERENCES

- (1) Macheleidt, J.; Mattern, D. J.; Fischer, J.; Netzker, T.; Weber, J.; Schroeckh, V.; Valiante, V.; Brakhage, A. A. *Annu. Rev. Genet.* **2016**, 50, 371–392.
- (2) Arias, M.; Santiago, L.; Vidal-Garcia, M.; Redrado, S.; Lanuza, P.; Comas, L.; Domingo, M. P.; Rezusta, A.; Galvez, E. M. *Front. Immunol.* **2018**, 9, 2549.
- (3) Sharpton, T. J.; Stajich, J. E.; Rounsley, S. D.; Gardner, M. J.; Wortman, J. R.; Jordan, V. S.; Maiti, R.; Kodira, C. D.; Neafsey, D. E.; Zeng, Q.; Hung, C. Y.; McMahan, C.; Muszewska, A.; Grynberg, M.; Mandel, M. A.; Kellner, E. M.; Barker, B. M.; Galgiani, J. N.; Orbach, M. J.; Kirkland, T. N.; Cole, G. T.; Henn, M. R.; Birren, B. W.; Taylor, J. W. *Genome Res.* **2009**, 19, 1722–1731.
- (4) Whiston, E.; Taylor, J. W. G3: Genes, Genomes, Genet. **2016**, 6, 235–244.
- (5) Yin, W. B.; Chooi, Y. H.; Smith, A. R.; Cacho, R. A.; Hu, Y.; White, T. C.; Tang, Y. *ACS Synth. Biol.* **2013**, 2, 629–634.
- (6) Harvey, C. J. B.; Tang, M.; Schlecht, U.; Horecka, J.; Fischer, C. R.; Lin, H. C.; Li, J.; Naughton, B.; Cherry, J.; Miranda, M.; Li, Y. F.; Chu, A. M.; Hennessy, J. R.; Vandova, G. A.; Inglis, D.; Aiyar, R. S.; Steinmetz, L. M.; Davis, R. W.; Medema, M. H.; Sattely, E.; Khosla, C.; St Onge, R. P.; Tang, Y.; Hillenmeyer, M. E. *Sci. Adv.* **2018**, 4, No. eaar5459.
- (7) Hilty, J.; George Smulian, A.; Newman, S. L. *Med. Mycol.* **2011**, 49, 633–642.
- (8) Hwang, L. H.; Mayfield, J. A.; Rine, J.; Sil, A. *PLoS Pathog.* **2008**, 4, No. e1000044.

- (9) Niu, S.; Si, L.; Liu, D.; Zhou, A.; Zhang, Z.; Shao, Z.; Wang, S.; Zhang, L.; Zhou, D.; Lin, W. *Eur. J. Med. Chem.* **2016**, *108*, 229–244.
- (10) Hosoe, T.; Iizuka, T.; Komai, S.; Wakana, D.; Itabashi, T.; Nozawa, K.; Fukushima, K.; Kawai, K. *Phytochemistry* **2005**, *66*, 2776–2779.
- (11) Wakana, D.; Hosoe, T.; Wachi, H.; Itabashi, T.; Fukushima, K.; Yaguchi, T.; Kawai, K. *J. Antibiot.* **2009**, *62*, 217–219.
- (12) Wakana, D.; Itabashi, T.; Kawai, K.; Yaguchi, T.; Fukushima, K.; Goda, Y.; Hosoe, T. *J. Antibiot.* **2014**, *67*, 585–588.
- (13) Fehlhaber, H. W.; Kogler, H.; Mukhopadhyay, T.; Vijayakumar, E. K.; Roy, K.; Rupp, R. H.; Ganguli, B. N. *J. Antibiot.* **1988**, *41*, 1785–1794.
- (14) Gamble, W. R.; Gloer, J. B.; Scott, J. A.; Malloch, D. J. *Nat. Prod.* **1995**, *58*, 1983–1986.
- (15) Hammerschmidt, L.; Aly, A. H.; Abdel-Aziz, M.; Muller, W. E.; Lin, W.; Daletos, G.; Proksch, P. *Bioorg. Med. Chem.* **2015**, *23*, 712–9.
- (16) Burmester, A.; Shelest, E.; Glockner, G.; Heddergott, C.; Schindler, S.; Staib, P.; Heidel, A.; Felder, M.; Petzold, A.; Szafranski, K.; Feuermann, M.; Pedrucci, I.; Priebe, S.; Groth, M.; Winkler, R.; Li, W.; Kniemeyer, O.; Schroeckh, V.; Hertweck, C.; Hube, B.; White, T. C.; Platzter, M.; Guthke, R.; Heitman, J.; Wostemeyer, J.; Zipfel, P. F.; Monod, M.; Brakhage, A. A. *Genome Biol.* **2011**, *12*, R7.
- (17) Desjardins, C. A.; Champion, M. D.; Holder, J. W.; Muszewska, A.; Goldberg, J.; Bailao, A. M.; Brigido, M. M.; Ferreira, M. E.; Garcia, A. M.; Grynberg, M.; Gujja, S.; Heiman, D. I.; Henn, M. R.; Kodira, C. D.; Leon-Narvaez, H.; Longo, L. V.; Ma, L. J.; Malavazi, L.; Matsuo, A. L.; Morais, F. V.; Pereira, M.; Rodriguez-Brito, S.; Sakthikumar, S.; Salem-Izacc, S. M.; Sykes, S. M.; Teixeira, M. M.; Vallejo, M. C.; Walter, M. E.; Yandava, C.; Young, S.; Zeng, Q.; Zucker, J.; Felipe, M. S.; Goldman, G. H.; Haas, B. J.; McEwen, J. G.; Nino-Vega, G.; Puccia, R.; San-Blas, G.; Soares, C. M.; Birren, B. W.; Cuomo, C. A. *PLoS Genet.* **2011**, *7*, No. e1002345.
- (18) Martinez, D. A.; Oliver, B. G.; Graser, Y.; Goldberg, J. M.; Li, W.; Martinez-Rossi, N. M.; Monod, M.; Shelest, E.; Barton, R. C.; Birch, E.; Brakhage, A. A.; Chen, Z.; Gurr, S. J.; Heiman, D.; Heitman, J.; Kosti, I.; Rossi, A.; Saif, S.; Samalova, M.; Saunders, C. W.; Shea, T.; Summerbell, R. C.; Xu, J.; Young, S.; Zeng, Q.; Birren, B. W.; Cuomo, C. A.; White, T. C. *mBio* **2012**, *3*, e00259–12.
- (19) Nielsen, J. C.; Grijseels, S.; Prigent, S.; Ji, B.; Dainat, J.; Nielsen, K. F.; Frisvad, J. C.; Workman, M.; Nielsen, J. *Nat. Microbiol.* **2017**, *2*, 17044.
- (20) Lin, Z.; Koch, M.; Abdel Aziz, M. H.; Galindo-Murillo, R.; Tianero, M. D.; Cheatham, T. E.; Barrows, L. R.; Reilly, C. A.; Schmidt, E. W. *Org. Lett.* **2014**, *16*, 4774–4777.
- (21) Lin, Z.; Phadke, S.; Lu, Z.; Beyhan, S.; Abdel Aziz, M. H.; Reilly, C.; Schmidt, E. W. *J. Nat. Prod.* **2018**, *81*, 2605–2611.
- (22) Blin, K.; Wolf, T.; Chevrette, M. G.; Lu, X.; Schwalen, C. J.; Kautsar, S. A.; Suarez Duran, H. G.; de Los Santos, E. L. C.; Kim, H. U.; Nave, M.; Dickschat, J. S.; Mitchell, D. A.; Shelest, E.; Breitling, R.; Takano, E.; Lee, S. Y.; Weber, T.; Medema, M. H. *Nucleic Acids Res.* **2017**, *45*, W36–W41.
- (23) Cimermanic, P.; Medema, M. H.; Claesen, J.; Kurita, K.; Wieland Brown, L. C.; Mavrommatis, K.; Pati, A.; Godfrey, P. A.; Koehrsen, M.; Clardy, J.; Birren, B. W.; Takano, E.; Sali, A.; Lington, R. G.; Fischbach, M. A. *Cell* **2014**, *158*, 412–421.
- (24) Chooi, Y. H.; Tang, Y. J. *Org. Chem.* **2012**, *77*, 9933–9953.
- (25) Finking, R.; Marahiel, M. A. *Annu. Rev. Microbiol.* **2004**, *58*, 453–488.
- (26) Boettger, D.; Hertweck, C. *ChemBioChem* **2013**, *14*, 28–42.
- (27) Kumar, S.; Stecher, G.; Tamura, K. *Mol. Biol. Evol.* **2016**, *33*, 1870–1874.
- (28) Medema, M. H.; Takano, E.; Breitling, R. *Mol. Biol. Evol.* **2013**, *30*, 1218–1223.
- (29) Adamek, M.; Spohn, M.; Stegmann, E.; Ziemert, N. *Methods Mol. Biol.* **2017**, *1520*, 23–47.
- (30) Shannon, P.; Markiel, A.; Ozier, O.; Baliga, N. S.; Wang, J. T.; Ramage, D.; Amin, N.; Schwikowski, B.; Ideker, T. *Genome Res.* **2003**, *13*, 2498–2504.
- (31) Capon, R. J. *Nat. Prod. Rep.* **2019**, DOI: 10.1039/C9NP00013E.
- (32) Halecker, S.; Surup, F.; Solheim, H.; Stadler, M. J. *Antibiot.* **2018**, *71*, 339–341.
- (33) Zhao, J.; Brosmer, J. L.; Tang, Q.; Yang, Z.; Houk, K. N.; Diaconescu, P. L.; Kwon, O. J. *Am. Chem. Soc.* **2017**, *139*, 9807–9810.
- (34) Moore, C.; Gupta, R.; Jordt, S. E.; Chen, Y.; Liedtke, W. B. *Neurosci. Bull.* **2018**, *34*, 120–142.
- (35) Ichihara, A.; Oikawa, H.; Hashimoto, M.; Sakamura, S.; Haraguchi, T.; Nagano, H. *Agric. Biol. Chem.* **1983**, *47*, 2965–2967.
- (36) Ugai, T.; Minami, A.; Fujii, R.; Tanaka, M.; Oguri, H.; Gomi, K.; Oikawa, H. *Chem. Commun.* **2015**, *51*, 878–881.
- (37) Gaucher, G. M.; Shepherd, M. G. *Biochem. Biophys. Res. Commun.* **1968**, *32*, 664–671.
- (38) Grumbt, M.; Monod, M.; Staib, P. *FEMS Microbiol. Lett.* **2011**, *320*, 79–86.
- (39) Kakule, T. B.; Jadulco, R. C.; Koch, M.; Janso, J. E.; Barrows, L. R.; Schmidt, E. W. *ACS Synth. Biol.* **2015**, *4*, 625–633.
- (40) Gottlieb, H. E.; Kotlyar, V.; Nudelman, A. J. *Org. Chem.* **1997**, *62*, 7512–7515.
- (41) Tianero, M. D.; Kwan, J. C.; Wyche, T. P.; Presson, A. P.; Koch, M.; Barrows, L. R.; Bugni, T. S.; Schmidt, E. W. *ISME J.* **2015**, *9*, 615–628.
- (42) Peng, Y.; Leung Hc Fau - Yiu, S. M.; Yiu Sm Fau - Chin, F. Y. L.; Chin, F. Y. *Bioinformatics* **2012**, *28*, 1420–1428.
- (43) Stanke, M.; Diekhans, M.; Baertsch, R.; Haussler, D. *Bioinformatics* **2008**, *24*, 637–644.
- (44) Aziz, R. K.; Bartels, D.; Best, A. A.; DeJongh, M.; Disz, T.; Edwards, R. A.; Formsma, K.; Gerdes, S.; Glass, E. M.; Kubal, M.; Meyer, F.; Olsen, G. J.; Olson, R.; Osterman, A. L.; Overbeek, R. A.; McNeil, L. K.; Paarmann, D.; Paczian, T.; Parrello, B.; Pusch, G. D.; Reich, C.; Stevens, R.; Vassieva, O.; Vonstein, V.; Wilke, A.; Zagnitko, O. *BMC Genomics* **2008**, *9*, 75.
- (45) Brettin, T.; Davis, J. J.; Disz, T.; Edwards, R. A.; Gerdes, S.; Olsen, G. J.; Olson, R.; Overbeek, R.; Parrello, B.; Pusch, G. D.; Shukla, M.; Thomason, J. A., 3rd; Stevens, R.; Vonstein, V.; Wattam, A. R.; Xia, F. *Sci. Rep.* **2015**, *5*, 8365.
- (46) Overbeek, R.; Olson, R.; Pusch, G. D.; Olsen, G. J.; Davis, J. J.; Disz, T.; Edwards, R. A.; Gerdes, S.; Parrello, B.; Shukla, M.; Vonstein, V.; Wattam, A. R.; Xia, F.; Stevens, R. *Nucleic Acids Res.* **2014**, *42*, D206–214.
- (47) Notredame, C.; Higgins, D. G.; Heringa, J. J. *Mol. Biol.* **2000**, *302*, 205–217.
- (48) Capella-Gutierrez, S.; Silla-Martinez, J. M.; Gabaldon, T. *Bioinformatics* **2009**, *25*, 1972–1973.
- (49) Chen, W. Z.; Fan, L. L.; Xiao, H. T.; Zhou, Y.; Xiao, W.; Wang, J. T.; Tang, L. *Chin. Chem. Lett.* **2014**, *25*, 749–751.
- (50) Zhu, J.; Porco, J. A., Jr. *Org. Lett.* **2006**, *8*, 5169–5171.